Efficient TEM_{00}-mode solar laser using four Nd:YAG rods/four off-axis parabolic mirrors pumping approach

Rabeh Boutaka,[a] **Dawei Liang**,[b,*] **and Abdelhamid Kellou**[c]
[a]Centre de Développement des Technologies Avancées, Alger, Algeria
[b]Universidade Nova de Lisboa, Departamento de Fisica, FCT, Lisboa, Portugal
[c]Université des Sciences et de la Technologie Houari Boumediene,
Département de Physique des Rayonnements, Faculté de Physique, Alger, Algeria

Abstract. A four-rod/four-TEM_{00}-mode beam off-axis parabolic mirror solar pumping concept is proposed. Four off-axis parabolic mirrors with 10 m^2 total collection area were used as the primary solar concentrators to pump four 3.1-mm diameter, 84-mm length neodymium-doped yttrium aluminum garnet (Nd:YAG) rods within four 2V-shaped pump cavities through four secondary fused-silica aspheric concentrators and four rectangular fused-silica light guides, ensuring a good absorbed pump power distribution within each rod and avoiding the serious thermal lensing and thermal stress issues associated with classical single large rod solar lasers. The laser design parameters were optimized using ZEMAX© and LASer Cavity Analysis and Design (LASCAD©) analysis software to maximize the TEM_{00}-mode laser power. 155.29-W TEM_{00}-mode total laser power was numerically calculated, corresponding to 15.5 W/m^2 solar laser collection efficiency and 1.72% solar-to-TEM_{00}-mode laser conversion efficiency, respectively. This result represents an improvement of nearly 2 and 1.24 times, in solar laser collection efficiency and solar-to-TEM_{00}-mode laser conversion efficiency, respectively, as compared with the previous experimental records of the TEM_{00}-mode solar laser pumped through the parabolic mirror primary concentrator. It provides also a 1.14 and 1.19 times improvement, as compared to the previous numerical record of the TEM_{00}-mode solar laser pumped by the Fresnel lens primary solar concentrator. © *2022 Society of Photo-Optical Instrumentation Engineers (SPIE)* [DOI: 10.1117/1.JPE.12.038002]

Keywords: TEM_{00}-mode; aspheric lens; light guide; side pumping; neodymium-doped yttrium aluminum garnet; off-axis parabolic mirror.

Paper 22012G received Feb. 20, 2022; accepted for publication Aug. 16, 2022; published online Sep. 6, 2022.

1 Introduction

The production of a laser light using solar energy as a pumping source has received significant attention in laser research since its first successful operation by Young in 1966.[1] The main reason for this attention may be explained by the abundance of free solar energy. Therefore, it can be used to produce a cost-effective laser system with the possibility of obtaining extremely high power and brightness, as compared to the conventional pumping sources such as flash lamps, laser diodes, and LEDs.

In the last decade, significant improvements in solar-pumped laser performances have been achieved for both multimode and fundamental-mode operations. In 2012, 120-W continuous-wave (CW) multimode solar laser power and a laser collection efficiency of 30 W/m^2 were achieved. In this work, a Fresnel lens solar concentration system with a large area of 4 m^2 was used to pump a 100-mm long neodymium-doped yttrium aluminum garnet (Nd:YAG) rod with a diameter of 6 mm.[2] In 2013, 2.3-W TEM_{00}-mode CW solar laser power was produced, corresponding to a TEM_{00}-mode collection efficiency of 2.93 W/m^2. In this work, a 3-mm diameter, 30-mm length Nd:YAG rod was pumped through a Fresnel lens concentration system with 0.785 m^2 collection area.[3] In 2016, 4.5-W TEM_{00}-mode CW solar laser power and 4-W/m^2 laser collection efficiency was achieved by pumping a 4-mm diameter, 34-mm length grooved

*Address all correspondence to Dawei Liang, dl@fct.unl.pt

Nd:YAG rod with a 1.13 m^2 effective area heliostat-parabolic mirror concentration system.[4] In 2017, a multimode solar laser power and collection efficiency of 37.2 W and 31.5 W/m^2, respectively, were measured by pumping a 35-mm long Nd:YAG rod with a diameter of 4 mm through a heliostat-parabolic mirror concentration system with 1.18-m^2 effective collection area.[5] In this work, 9.3-W TEM_{00}-mode solar laser power and 7.9-W/m^2 record TEM_{00}-mode collection efficiency was also registered. In 2018, a large composite Nd:YAG rod was pumped through a Fresnel lens with an area of 1.03 m^2 to obtain a multimode solar laser power of 33.1 W and a corresponding laser collection efficiency of 32.1 W/m^2.[6] In the same year, a multimode solar laser power of 32.5 W and the record multimode collection efficiency equal to 32.5 W/m^2 were achieved by pumping a 4-mm diameter, 35-mm length Cr:Nd:YAG ceramic rod through a heliostat-parabolic mirror concentration system. A record solar-to-laser power conversion efficiency of 3.74% was also registered in this work.[7] Recently, a numerical study of multi-beam Fresnel lens solar laser pumping concept was proposed in 2021.[8] In this study, a total TEM_{00}-mode solar laser power of 54.65 W was calculated by pumping seven 2.5-mm diameter, 15-mm length Nd:YAG rods within a conical pump cavity through 4-m^2 primary Fresnel lens concentrator collection area, corresponding to TEM_{00}-mode solar laser collection efficiency of 13.66 W/m^2 and solar to-TEM_{00}-mode laser conversion efficiency of 1.44%. In this work, it has been confirmed that the improvement in fundamental-mode laser output power can be attained by pumping several small diameter laser rods simultaneously within a single laser head and using large-mode volume resonator configuration.

Now, solar lasers can be used in numerous applications, such as high-temperature material processing and the magnesium-hydrogen energy cycle.[9–15]

Among the potential applications of solar lasers are earth, ocean, and atmospheric sensing; laser beaming; deep space communications; space debris removal.[13,16–20] Since solar energy is the most available and reliable power source in space, space-based solar power generation, which is 10 times more efficient than Earth-based, would be a major step forward in terms of fulfilling energy needs, as the strength of sunlight in space is about twice that on Earth, and there are four or five times the hours of sunlight due to the complete absence of clouds.

A significant shortcoming of semiconductor laser arrays is their limited life time and performance degradation over time, which seems to scale with the level of average output power. For high-power laser systems, the lifetime of these devices is one of the major factors limiting the lifetime of a laser system or even an entire system to the order of round about 10,000 h. Entirely avoiding semiconductor laser arrays by direct solar pumping of solid-state lasers exhibits its potential to overcome the current limitations, enabling reliable space borne laser operation over a multitude of years. Terrestrial applications may become more obvious if an efficient renewable TEM_{00}-mode laser with excellent beam profile can be operational in many Sun-rich countries.

To avoid shortcomings, such as thermal lensing and thermal stress, a single-laser/multi-TEM_{00}-mode beams solar laser pumping approach using four off-axis parabolic mirrors is proposed here. This approach has also high compactness since one laser serves many fundamental-mode laser spots, each precisely controllable with a minimum heat input on each of many thin laser rods within a single pump cavity, thus, providing the capability to tailor the applied energy to the specific needs for laser material processing applications.[21–25]

The four off-axis mirrors with 10-m^2 total collection area were used as the primary solar concentrators to collect and concentrate the incoming solar rays toward a single laser head, within which a four 3.1-mm diameter, 84-mm length Nd:YAG rods were side-pumped simultaneously through a four secondary fused-silica aspheric concentrators and four 2V-shaped pump cavities, ensuring an efficient coupling of the concentrated solar power from the four focal zones of the off-axis parabolic mirrors into the four laser rod. Four rectangular-shaped fused-silica light guides were also used to ensure a good absorbed pump power distribution within each rod. All the laser design parameters were optimized using ZEMAX© non-sequential ray-tracing and LASCAD© laser-cavity analysis software to maximize the TEM_{00}-mode laser power. A significant improvement in the TEM_{00}-mode output power level, collection efficiency, and solar-to-laser power conversion efficiency through numerical calculations was achieved. About 155.29-W TEM_{00}-mode total laser power was calculated, corresponding to 15.5-W/m^2 solar laser collection efficiency and 1.72% solar-to-TEM_{00}-mode laser conversion efficiency, respectively. This result represents an improvement of 1.96 and 1.24 times, in solar laser collection efficiency and solar-to-TEM_{00}-mode laser conversion efficiency respectively, as compared with the previous experimental records of the TEM_{00}-mode solar laser pumped through the parabolic mirror primary concentrator.[5] It offers also a 1.14 and 1.19 times improvement, in solar laser collection efficiency and solar-to-TEM_{00}-mode laser conversion efficiency respectively, as compared to previous numerical record of the TEM_{00}-mode solar laser pumped by the Fresnel lens primary solar concentrator.[8]

2 ZEMAX© and LASCAD© Optimization of the TEM_{00}-Mode Solar Laser System

2.1 *ZEMAX© and LASCAD© Description*

The design parameters of all the solar pumping system were first optimized using the non-sequential ray-tracing method of ZEMAX© software.[26] Then, the laser resonator parameters were modeled by LASer Cavity Analysis and Design (LASCAD©) codes to optimize the laser output power and beam quality.[27] The non-sequential method of ZEMAX© is used for optical systems, which are non-imaging. In this method, the rays are traced only along a physically realizable path until they intercept an object. The rays are then refracted, reflected, or absorbed by the object, and continue on a new path. The detectors objects define the qualitative and/or quantified information of the incident rays. In ZEMAX© software, several parameters must be inserted such as the geometry and position of all elements, the source power and wavelength, the source rays distributions, the types of each element used and its optical properties, etc.

The LASCAD© software allows the combination of several simulation tools to optimize the laser resonator design: the thermal and structural finite element analysis, the ABCD Gaussian beam propagation code, and the propagation algorithm of non-Gaussian beams—the beam propagation method (BPM). Thus, it is possible to model resonant cavities through the analysis of: the thermal lensing effects, which is one of the key problems in solid-state lasers; multimode and TEM_{00}-mode output power and laser efficiency; laser beam quality and profile, as well as laser beam propagation outside the laser cavity, taking into account several laser parameters, such as reflectivity, radius of curvature (RoC) and distance between cavity components, diffraction losses, gain saturation etc.

2.2 *Solar Energy Collection and Concentration System*

The solar energy collection and concentration system used to side-pump four Nd:YAG rods is shown in Figs. 1(a) and 1(b). This system was optimized by ZEMAX© software in our previous work[28] and was composed of four off-axis parabolic mirrors ($M_1 - M_4$), serving as primary concentrators. Each mirror has 1.785-m diameter, 1.35-m focal length, and provided an effective solar collection area of 2.5 m^2. Thus, the total collection area of the four primary concentrators was 10 m^2. A protective silver primary mirror coating with 95% reflectivity was also assumed for the numerical analyses.

The off-axis parabolic mirror design completely eliminated the shadowing effect of the laser head and its associated fixing mechanics, compared to the conventional heliostat-parabolic mirror systems. A detailed description of the laser head shown in Fig. 1(c) is provided in Sec. 2.3.

The center of each parabolic mirror was positioned 1350 mm away from their common center point C in either the X- or Z-axis directions. All mirrors were tilted at a 45-deg angle, relative to the Y-axis. About 18-mm shifts between each two neighboring mirrors along the Y-axis was considered to provide the correct solar light couplings from the focal spots of the four off-axis parabolic mirrors to the Nd:YAG rods through aspheric fused-silica lenses and rectangular fused-silica light guides. Assuming an average terrestrial solar irradiance of 950 W/m^2 on clear sunny days, and 95% reflectivity of the primary concentrators, a solar power of 2256 W can be focused within a near Gaussian light spot of $\sim$11 mm full width at half maximum diameter for each 2.5 m^2 area off-axis parabolic mirror, as shown in Fig. 2. Consequently, a total solar power

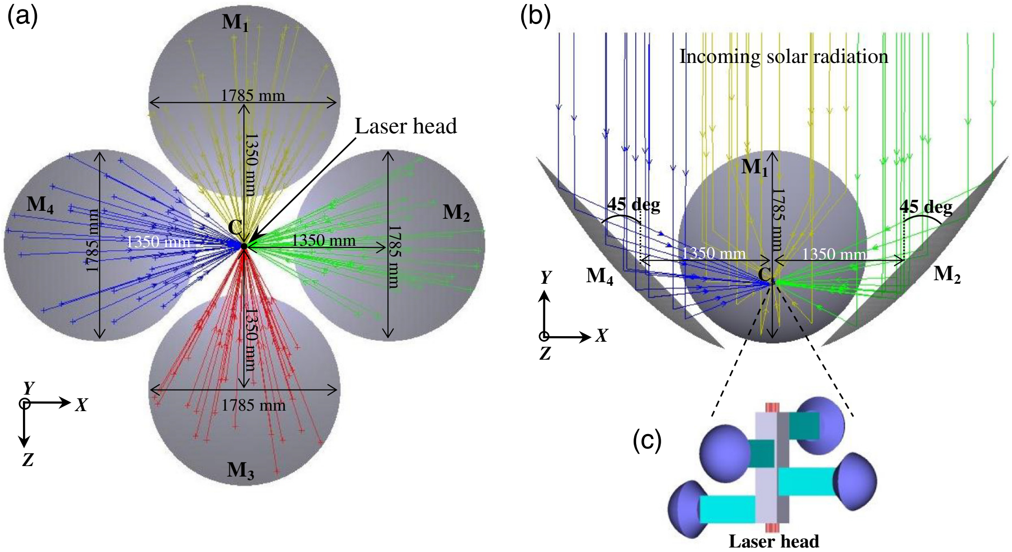

Fig. 1 Simplified scheme of a side-pumped solar laser system with four off-axis parabolic mirrors: (a) front-view; (b) side-view without mirror M_3 to illustrate how incoming solar rays are focused toward the laser head; and (c) inset figure of the laser head mounted at the common center point C of the four off-axis parabolic mirrors.

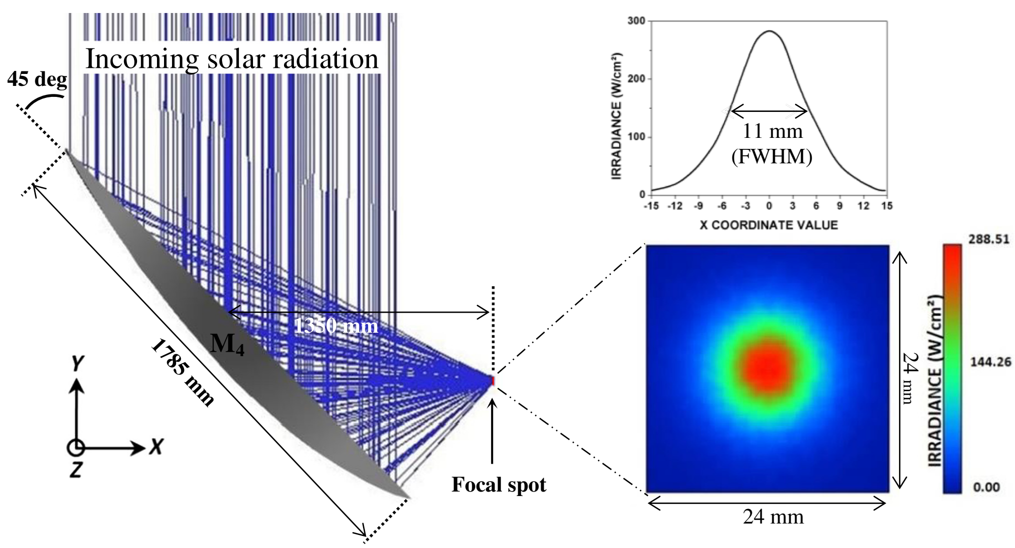

Fig. 2 Spatial distribution of the concentrated solar light at the off-axis mirror focal zone obtained through ZEMAX© analysis.

of 9025 W for the four parabolic mirrors with a total collection area of 10 m^2 was assumed to reach the large input faces of the four fused-silica secondary concentrators shown in Fig. 1(c).

2.3 *Solar Laser Head with Four Fused-Silica Aspheric Lenses, Four Rectangular Fused-Silica Light Guides, Four 2V-Shaped Pump Cavities and Four Nd:YAG Rods*

As shown in Fig. 3(a), the solar laser head was composed of four fused-silica aspheric lenses (L_1–L_4) used as secondary concentrators, four fused-silica light guides with rectangular-shaped cross section (G_1–G_2) served as a solar power homogenizer, and four 2V-shaped pump cavities

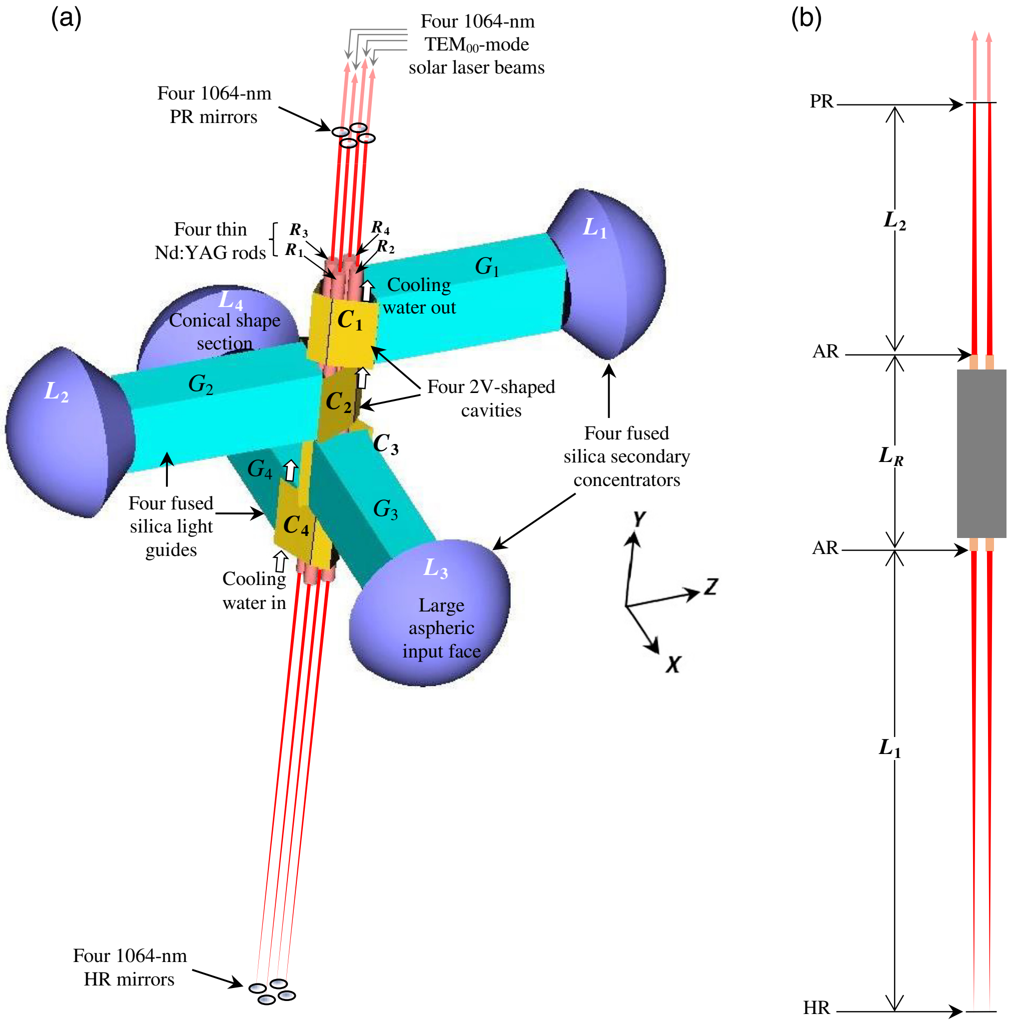

Fig. 3 (a) 3D view and (b) 2D view of the solar laser head design for the TEM_{00}-mode solar laser operation, composed of four fused-silica aspheric lenses, four rectangular fused-silica light guides, four 2V-shaped pump cavities, and four asymmetric resonant cavities. Each asymmetric resonant cavity was composed of a thin Nd:YAG laser rod with both end faces 1064-nm antireflection coated (AR), a 1064-nm HR end mirror, and a 1064-nm PR output coupler.

(C_1–C_4), wherein a four thin Nd:YAG rods (R_1–R_4) with a length (L_R) of 84 mm and a diameter (D_R) of 3.1 mm were pumped and water cooled.

As the adoption of an asymmetric resonator may provide a large spatial overlap between the fundamental laser mode volume and the solar pump volume,[3,5] an asymmetric resonant cavity with two concave end mirrors was used in LASCAD© analyses for extracting the maximum TEM_{00}-mode laser power from each Nd:YAG rod, as shown in Figs. 3(a) and 3(b).

Each asymmetric resonator has a high reflection (HR)-coated rear mirror (HR, 99.98% at 1064 nm) and a partial reflection (PR)-coated output mirror (PR at 1064 nm). Both HR and PR mirrors were aligned near the thermal focal zone of the rod to achieve maximum extraction of TEM_{00}-mode 1064-nm laser power with Gaussian profiles. L_1 and L_2 represent the separation length from the anti-reflection coating (AR1064 nm) end faces of the laser rod to the HR1064-nm rear mirror and to the PR1064-nm output mirror, respectively. L_1 and L_2 are the key parameters for achieving the highest TEM_{00}-mode laser power. The resonator length L varied according to the rod diameter (D_R) and the RoC of the two mirrors.

As shown in Fig. 4(a), each fused-silica lens had an aspheric input face with a diameter of 38 mm, a RoC of 20 mm, and a rear conic parameter r^2 of –0.005. The other side is a conical shape section with a diameter of 20 mm of the plane output face. A total lens thickness is 25 mm.

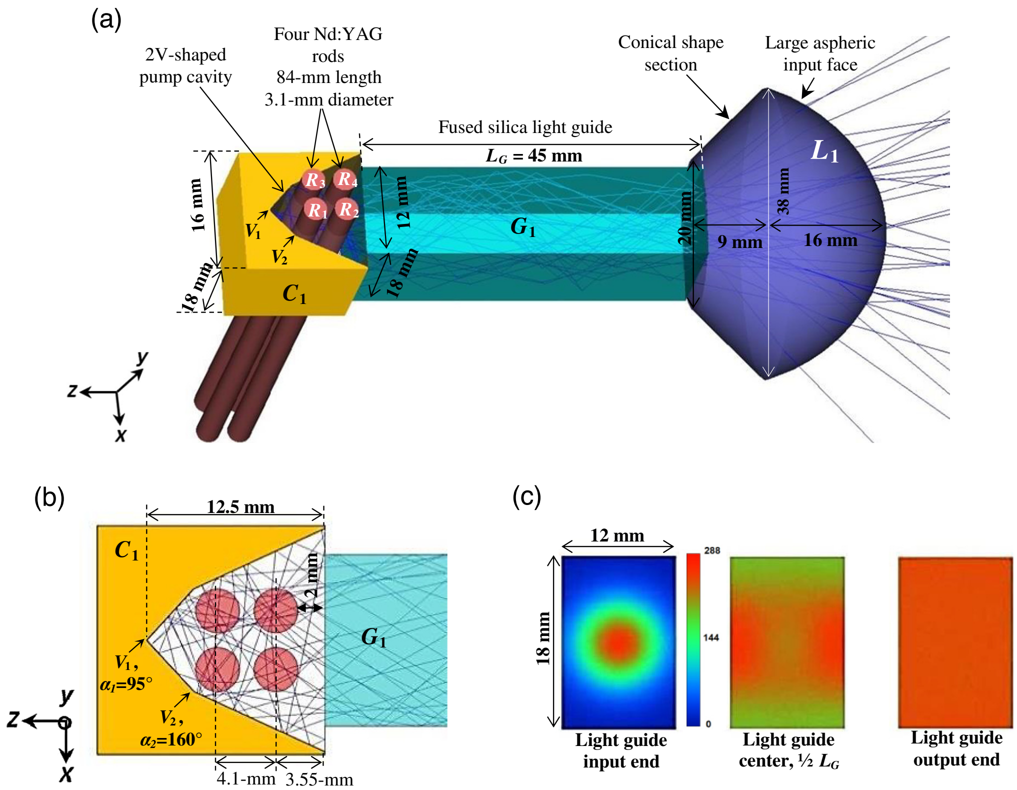

Fig. 4 (a) Solar pumping scheme of one of the four fused-silica aspheric lenses (L_1), one rectangular-shaped fused-silica light guide (G_1), and one 2V-shaped pump cavity (C_1); (b) side-view of the 2V-shaped pump cavity (C_1); and (c) solar radiation distribution inside the rectangular fused-silica light guide.

The solar radiation first concentrated by the each aspheric lens is then collected by a rectangular fused-silica light guide. This component was optimized by ZEMAX© software to 18 mm × 12 mm cross section and 45-mm length.

The rectangular fused silica light guide behaves like a beam homogenizer by transforming the near-Gaussian profile at its input end to a uniform pump light distribution at its output end, as shown in Fig. 4(c). Enabling hence a homogeneous absorbed pump light distribution along the Nd:YAG laser rods. This helps not only to reduce the thermal effects in the laser rod but also to compensate the heliostat tracking error dependent losses, leading to higher solar laser beam stability compared to solar lasers with no light homogenizer.[29] For example, when a light guide with a circle cross section is used, the solar radiation distribution obtained by ZEMAX at the output end of the guide remains near-Gaussian (non-uniform) similar at its input end. The choice of the fused-silica material for both the aspheric lenses and the light guides is for the reason that this material is an ideal optical one for Nd:YAG solar laser pumping, as it is transparent over the Nd:YAG absorption spectrum and has good optical and thermal properties, such as a high energy damage threshold[30] and high transmission efficiency of light.[29]

As shown in Fig. 4(b), each 2V-shaped pump cavity was fixed near the output end face of the rectangular fused-silica light guide. It was composed of a V-shaped reflector V_1 at an angle $\alpha_1 = 95$ deg, and two upper plane reflectors V_2 at an angle $\alpha_2 = 160$ deg. The entrance aperture was 16 mm × 18 mm, with a depth of 12.5 mm. The inner wall of the cavity was bonded with a protected silver-coated aluminum foil with 94% reflectivity. This 2V-shaped pump cavity ensured efficient coupling of the concentrated light exiting the output end face of the rectangular light guide to the four laser rods. As shown in Fig. 4(b), large portion of the pump rays were directly focused onto the exterior surface of the laser rods. The remaining pump rays, without passing directly through the rods, were also efficiently coupled to the laser mediums through zigzag reflections by the pump cavity inner walls. Consequently, efficient pump absorption by the four rods was achieved.

More importantly, pumping several small diameter rods simultaneously can eliminate the problem of incomplete absorption of solar pump energy, as compared with the previous single rod scheme.[28] It allows also achieving a very effective rod cooling, reducing hence the thermal lensing and thermal stress problems which may affect directly the laser output performances.[2,31] The water flow directions in the four pump cavities are shown in Fig. 3(a) by the white arrows, a flow rate of 6 l/min was considered in the calculations.

2.4 *ZEMAX© Optimization of the Absorbed Pump Power for TEM_{00}-Mode Operation*

Similar to the previous numerical analysis on solar lasers[3–5,7,8,28,32,33] all the above mentioned design parameters of the solar laser system in Figs. 1–4 were first optimized by non-sequential ray-tracing ZEMAX© software to achieve the maximum absorbed pump power with the best pump distribution possible inside the four Nd:YAG single-crystal rods. A total of 22 absorption peak wavelengths of 1% at. Nd^{3+}-doped YAG single-crystal rod and their respective absorption coefficients were added to the glass catalogue in the ZEMAX© software.[34] The absorption spectra and refractive indexes of fused-silica and water were also defined in the ZEMAX© numerical data. The 16% overlap coefficient between the Nd:YAG absorption spectrum and the solar spectrum was considered for the effective pump power of the solar source.[35] Despite this small overlap value, several studies have confirmed that Nd:YAG is the best material for solar pumping owing to its good thermal conductivity, high quantum efficiency, and high mechanical strength compared to other host materials.[36–40] For the ray-tracing analysis of the absorbed pump power and respective pump intensity distribution within the laser media, a detector volume divided into 18,000 zones was used for each laser rod. During ray-tracing, the path length of the rays through each zone was determined and then the absorbed pump power in each zone was found. The total absorbed pump power for each laser rod was finally calculated by summing the absorbed pump power of all zones. Figure 5 shows the pump-flux distributions of the absorbed pump power obtained by ZEMAX© software along the central longitudinal cross section and four transversal cross-sections of each Nd:YAG laser rod (R_1–R_4). The red color indicates near maximum pump absorption, whereas blue indicates little or no absorption. As expected, due to the no symmetry of the pump cavities positions in relation to each rod, no-identical absorbed pump profiles were observed inside the four rods, as shown by the central longitudinal cross sections. However, the calculated absorbed pump power was slightly different from a rod to another; it was 233.1 W for the rod R_1, 242.2 W for R_2, 234.1 W for R_3, and 240.9 W for R_4.

As illustrated by the transversal cross-section of each Nd:YAG laser rod, a quasi-uniform pump distribution was achieved inside the four laser rods within each pump cavity, ensuring the maximum absorbed pump power by the four rods and providing the maximum TEM_{00}-mode laser output power. Moreover, these pump profiles may considerably reduce the thermal effects within the rods, often encountered when the absorption profile is centrally peaked,[32,41] increasing hence the solar laser output performance.

2.5 *LASCAD© Analyses for the Maximum Extraction of Four TEM_{00}-Mode Beams*

The absorbed pump flux data obtained by ZEMAX© analysis was then processed using the LASCAD© software to optimize and calculate the solar laser output parameters for each rod such as the solar laser output power, the collection efficiency, and the laser beam quality. Various parameters of the 1% at. Nd:YAG active medium were also defined in LASCAD© software such as the stimulated emission cross section of 2.8×10^{-19} cm^2, the fluorescence lifetime of 230 μs, the typical absorption and scattering losses of 0.003 cm^{-1}, and the average absorbed and intensity-weighted solar pump wavelength of 660 nm.[42]

Figure 6 shows the asymmetric resonant cavity used in LASCAD© analyses for extracting the maximum TEM_{00}-mode laser power from the Nd:YAG rod R_1.

The separation lengths L_1 and L_2 were optimized by LASCAD© at 456 and 156.3 mm, respectively, to achieve the best overlap between the pump volume and the fundamental-mode

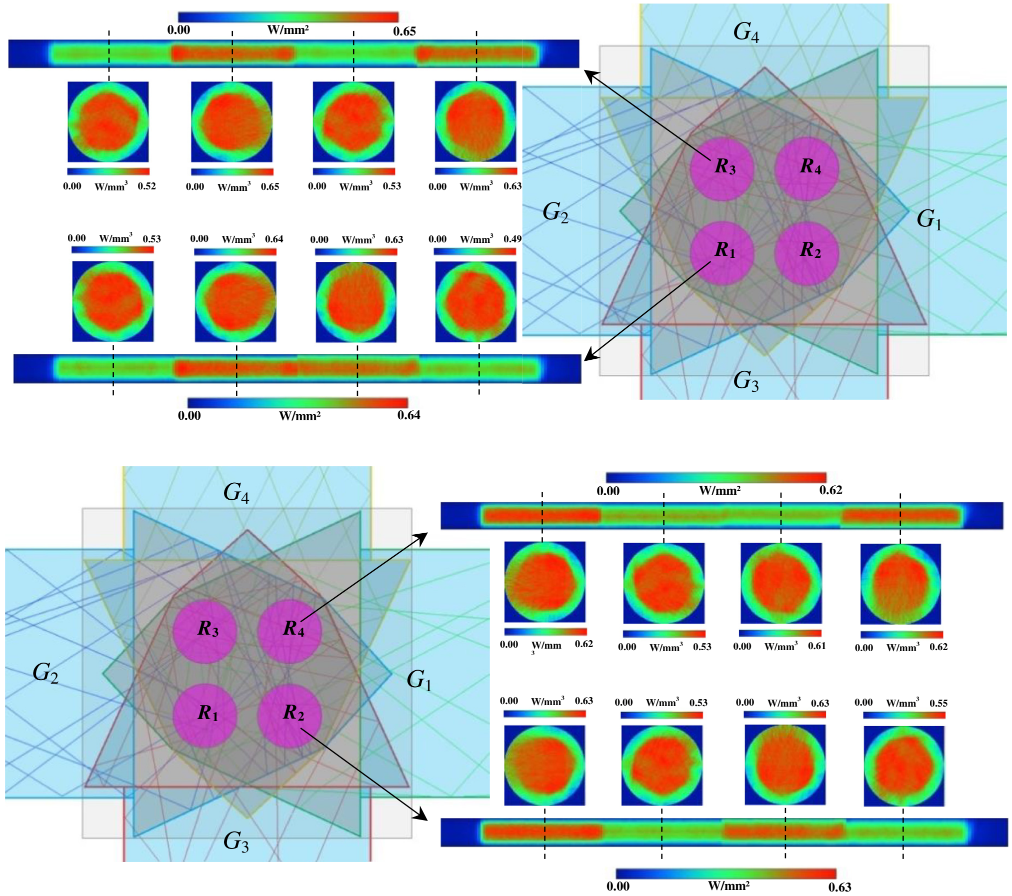

Fig. 5 ZEMAX© optimization of the Absorbed pump-flux distributions inside the four 3.1-mm diameter, 84-mm length Nd:YAG rods (R_1 – R_4).

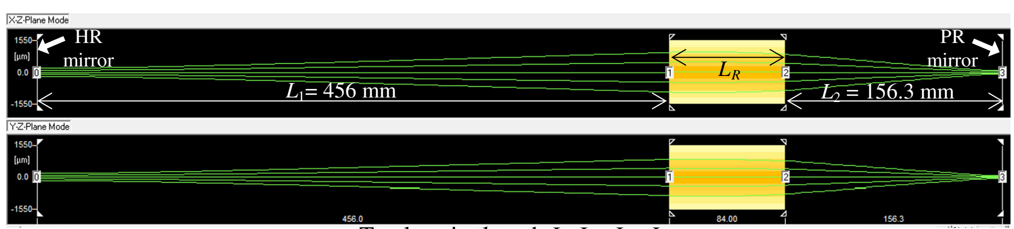

Fig. 6 LASCAD© representation of the asymmetric laser resonant cavity for the maximum TEM$_{00}$-mode laser power extraction from Nd:YAG rod R_1.

volume. As shown in Fig. 7, the maximum TEM$_{00}$-mode laser power for the rod R_1 was attained with a RoC $= 0.75$ m for both HR and PR mirrors.

As the amount of feedback is determined by the reflectivity (R) of the PR output coupler, different reflectivity values were tested individually to optimize the TEM$_{00}$-mode solar laser power for each rod. Figure 8 shows the evolution of the TEM$_{00}$-mode laser power of the rod R_1 as a function of the output coupler reflectivity.

The maximum TEM$_{00}$-mode laser power of 41.4 W was achieved for an output coupler reflectivity $R = 0.86$. As illustrated in Fig. 9(a), a near-Gaussian profile was verified at the output coupler of the rod R_1. The beam waist was calculated by the BPM cavity iterations method of LASCAD© software. Figure 9(b) shows that the $1/e^2$ width beam waist value

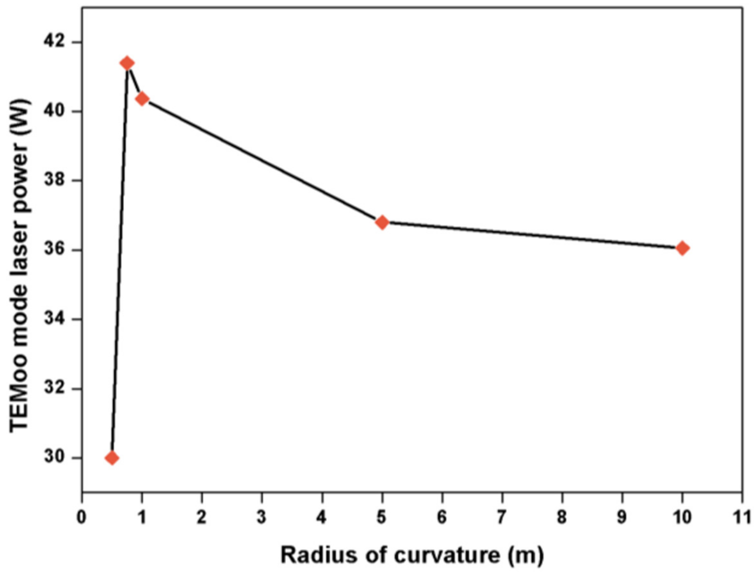

Fig. 7 Evolution of the TEM_{00}-mode solar laser power of the rod R_1 as a function of the RoC of both HR and PR mirrors.

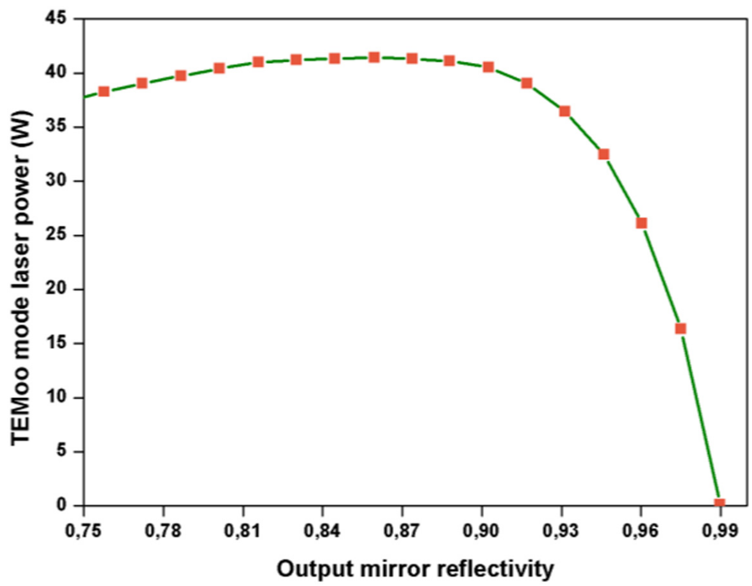

Fig. 8 Evolution of the TEM_{00}-mode solar laser power of the rod R_1 as a function of the PR mirror reflectivity.

stabilized at $\omega = 67$ μm after 150 iterations. The laser beam quality factor was calculated to be $M_x^2 = 1.53$ and $M_y^2 = 1$, and about 0.86% diffraction loss was also calculated by the BPM analysis.

The resonant cavities used for the other Nd:YAG rods (R_1, R_2, and R_3) were identical in principle to the rod R_1. Therefore, LASCAD© calculations were approximately similar to R_1. Table 1 summarizes the numerical results obtained for the other rods:

The maximum total TEM_{00}-mode solar laser power of 155.29 W was then calculated by summing up the TEM_{00}-mode powers extracted from the four Nd:YAG rods. Figure 10 summarizes the calculated results for each rod.

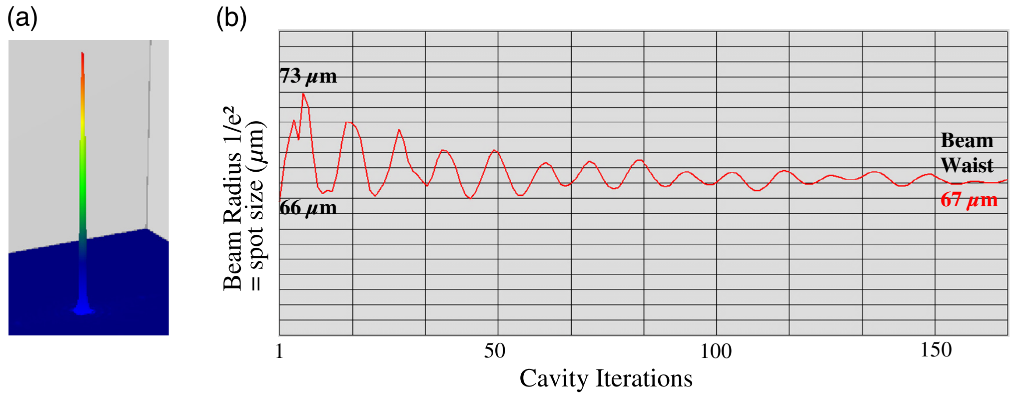

Fig. 9 (a) TEM$_{00}$-mode output beam profile of rod R_1 and (b) laser beam waists at output mirror calculated by BPM cavity iterations.

Table 1 Summary of the numerical results of the resonator lengths (L_1 and L_2), the M_x^2, M_y^2 beam quality factors, the RoC of both HR and PR mirrors, and the PR mirror reflectivity (R) for each one of the four 3.1-mm diameter and 84-mm length Nd:YAG rods.

Nd:YAG rod	L_1 (mm)	L_2 (mm)	RoC (m)	R (%)	ω (μm)	M_x^2	M_y^2	Diffraction loss (%)
R_2	456	157.3	0.75	0.87	68.3	1.00	1.35	0.8
R_3	456	165.5	0.75	0.87	70.9	1.00	2.47	1.1
R_4	456	167.6	0.75	0.88	70.1	1.00	1.23	1.1

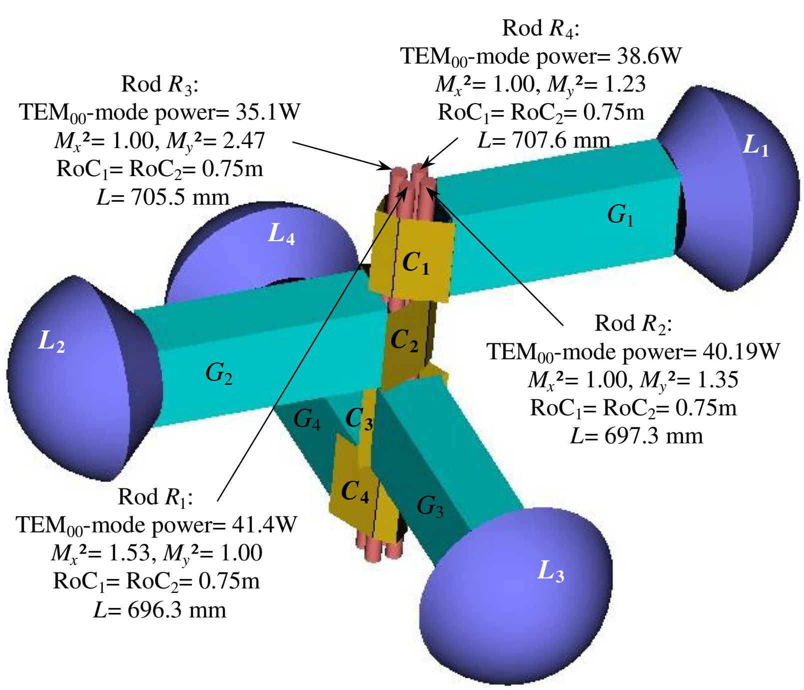

Fig. 10 Summary of the numerical results of the TEM$_{00}$-mode power, the M_x^2, M_y^2 beam quality factors, the RoC of both HR and PR mirrors, and the resonator length (L) for each one of the four 3.1-mm diameter and 84-mm length Nd:YAG rods.

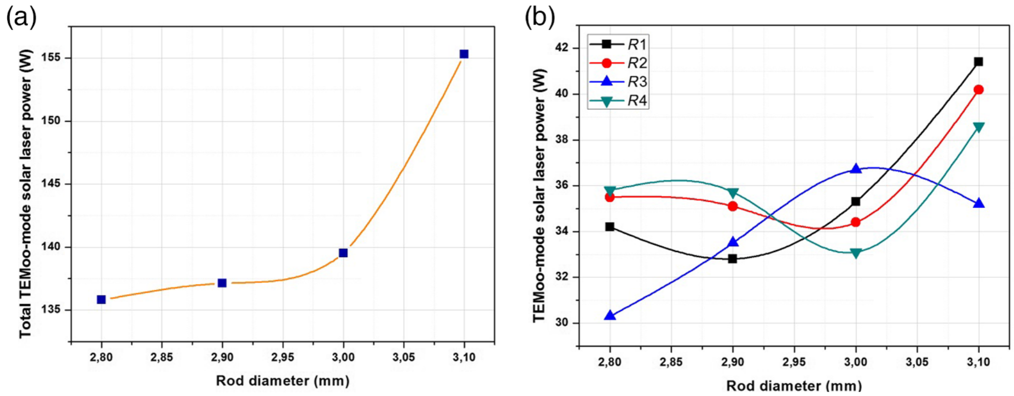

Fig. 11 TEM_{00}-mode laser power as a function of the rod diameter: (a) total TEM_{00}-mode laser power extracted from the four rods, and (b) TEM_{00}-mode laser power extracted from each rod.

2.6 *Numerical Optimization of TEM_{00}-Mode Laser Power from the Four Nd:YAG Rods*

All the design parameters of the off-axis parabolic mirror solar laser (pump cavities, rods dimensions and resonators) were optimized through ZEMAX© and LASCAD© numerical analysis software to achieve the highest fundamental-mode laser power from each laser rod. The laser rod diameter (D_R) was one of the most important design parameters for attaining the maximum TEM_{00}-mode solar laser power. Therefore, the TEM_{00}-mode laser power from each one of the four rods was numerically studied as a function of the laser rod diameter, as represented in Fig. 11. The 3.1-mm rod diameter was found as the optimum diameter value. By increasing the rods diameter above 3.1 mm, we observed that it is not possible to produce a TEM_{00}-mode solar laser for all the four rods (large M^2 factors have been obtained). Only the Nd:YAG rod R_3 has the maximum TEM_{00}-mode power with a 3-mm diameter, as shown in Fig. 11(b). However, the total TEM_{00}-mode laser power was decreased by about 15 W for the four rods with 3-mm diameter, as compared by the 3.1-mm rod diameter, as shown in Fig. 11(a).

Pumping small diameter rod is very attractive but challenging for solar laser researchers. Minimizing a laser rod volume reduces cost, and reducing the diameter makes the rod more resistant to thermal stress. More importantly, with smaller rod, laser beam M^2 factors can be significantly reduced, as compared to that from a large diameter laser rod.

The absorption, scattering, and diffraction losses for 1064-nm laser emission wavelength within the active medium constituted the most important part of round-trip resonant cavity losses. Imperfect HR and AR coating losses of the resonator cavity mirrors and the laser media was also an important portion of the round-trip losses.[3,5] For the four 1 at% Nd:YAG rods with 3.1-mm diameter (D_R) and 84-mm length (L_R), the amount of absorption and scattering losses was $2\alpha L_R = 5.04\%$. Assuming 0.4% of imperfect HR and AR coating losses, the round-trip loss increased to 5.44% for each rod. The diffraction loss, which depends heavily on the rod diameter

Table 2 Summary of the numerical results of the laser cavity losses for each one of the four Nd:YAG rods.

Nd:YAG rod	Diffraction loss calculated by BPM (%)	Absorption and scattering losses (%)	Imperfect HR and AR coating losses (%)	Total round-trip loss (%)	Maximum TEM_{00}-mode laser power (W)
R_1	0.86	5.04	0.4	6.3	41.4
R_2	0.8	5.04	0.4	6.24	40.19
R_3	1.1	5.04	0.4	6.54	35.1
R_4	1.1	5.04	0.4	6.54	38.6

and the RoC of the HR and PR mirrors, was calculated numerically by the LASCAD© BPM. Table 2 summarizes the cavity losses calculations for the four Nd:YAG rods

3 Discussion

The four individual TEM$_{00}$-mode laser beams in Fig. 3 can be merged into one single TEM$_{00}$-mode laser beam using several folding mirrors, as shown in Fig. 12. The novel laser beam merging resonant cavity was composed of a PR 1064-nm output mirror, the four thin laser rods, three sets of two-folding-mirrors ($FM_1 - FM_6$), and an HR 1064-nm end mirror. As mentioned by our previous work on laser beam merging technique for a four-rod lamp-pumped laser,[43] the folding-mirrors played an important role in improving the final laser output beam quality factors M_x^2, M_y^2. The inset of Fig. 12 shows how the plane folding mirrors were used to achieve a single laser beam with enhanced quality factors. The first (FM_1 and FM_2) and the third (FM_5 and FM_6) were composed of HR 1064-nm folding mirrors and inclined at 45-deg angle relative to the Z-axis. The second set (FM_3 and FM4) was composed of an HR 1064-nm mirror and inclined at 45-deg angle relative to the X-axis. Through this resonator design, the merged TEM$_{00}$-mode laser beam profile can be a more symmetric Gaussian profile.

A total TEM$_{00}$-mode laser power of 155.29 W (41.4 W+40.19 W+35.1 W+38.6 W) was then calculated. With 10-m^2 total solar collection area of the four primary off-axis parabolic concentrators, a corresponding TEM$_{00}$-mode solar laser collection efficiency of 15.5 W/m^2 and a solar-to-TEM$_{00}$-mode laser conversion efficiency of 1.72% were calculated at solar irradiance of 950 W/m^2. This result represents an enhancement of 1.96 and 1.24 times, as compared with the previous experimental records of the TEM$_{00}$-mode solar laser end-side-pumped through the parabolic mirror primary solar concentrator at 1010 W/m^2 of solar irradiance.[5] It represents also 5.29 and 5.24 times higher than the previous experimental records of the TEM$_{00}$-mode solar laser pumped by the Fresnel lens at 890W/m^2 of solar irradiance.[3] Solar TEM$_{00}$-mode collection efficiency and solar-to-TEM$_{00}$-mode laser power conversion efficiency was also enhanced by 3.78 and 2.35 times, respectively, as compared with the previous experimental records of the TEM$_{00}$-mode solar laser side-pumped through the parabolic mirror primary solar concentator.[4] Moreover, our result obtained herein is 1.14 and 1.19 times higher than the previous numerical

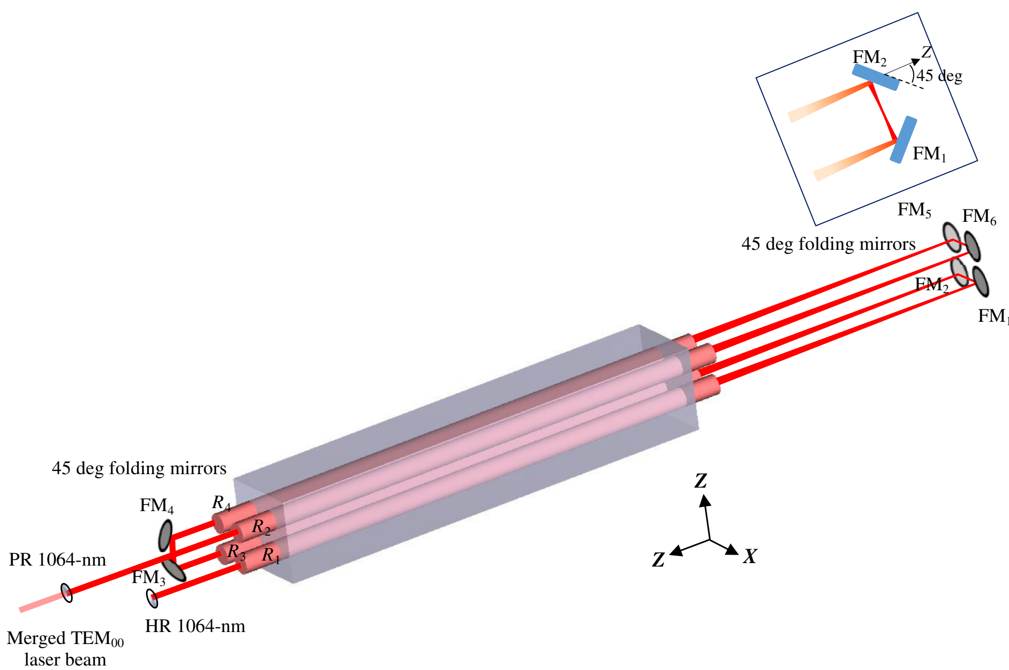

Fig. 12 TEM$_{00}$-mode laser beams merging method by a resonant cavity composed of an PR 1064 nm output mirror, four thin laser rods, folding-mirrors, and an HR 1064-nm end mirror.

records, in solar laser collection efficiency and solar-to-TEM_{00}-mode laser conversion efficiency respectively, for the TEM_{00}-mode solar laser pumped by the Fresnel lens primary solar concentrator.[8]

4 Conclusions

Herein, an efficient TEM_{00}-mode Nd:YAG solar laser side-pumped by four 2.5-m^2 area primary off-axis parabolic concentrators was numerically investigated. The ZEMAX© and LASCAD© software were used to optimize four TEM_{00}-mode laser beams produced simultaneously by four 3.1-mm diameter, 84-mm length Nd:YAG rods, enclosed within four 2V-shaped pump cavities. Four secondary fused-silica aspheric concentrators were used to efficiently concentrate the solar rays from the focal zones of the primary off-axis parabolic concentrators toward laser rods. Four rectangular fused-silica light guides were also employed to homogenize the pump distribution profiles along the laser rods and to enhance the tracking error compensation capacity. The proposed four-rod/four-beam TEM_{00}-mode solar laser pumping approach reduced considerably the problem of incomplete absorption of solar pump power by a single thin laser rod, such as observed in the previous works.[3] Moreover, efficient pump light absorption and effective laser rods cooling were achieved, reducing significantly the thermal effects inside the laser active mediums, which may affect directly the large-diameter-rod solar lasers performances.

Four TEM_{00}-mode CW laser beams 1064 nm with a maximum total power of 155.29 W was numerically calculated, corresponding to solar laser collection efficiency and solar-to-TEM_{00}-mode laser conversion efficiency of 15.5 W/m^2 and 1.72%, respectively. This result represents an improvement of nearly 2 and 1.24 times, in solar laser collection efficiency and solar-to-TEM_{00}-mode laser conversion efficiency respectively, as compared with the previous experimental records of the TEM_{00}-mode solar laser pumped through the parabolic mirror primary solar concentrator.[5] It provides also a 1.14 and 1.19 times, respectively, higher than the previous numerical record of the TEM_{00}-mode solar laser pumped by the Fresnel lens primary solar concentrator.[8] The results obtained herein can be used to implement a powerful solar laser station capable of producing several hundred watts of power in both TEM_{00}-mode and multimode operations.

Acknowledgments

Financial support for the Strategic Project UID/FIS/00068/2020 of the Science and Technology Foundation of Portuguese Ministry of Science, Technology, and Higher Education (FCT-MCTES) is gratefully acknowledged. The fellowship grant of Rabeh Boutaka from the Algerian Ministry of Higher Education and Scientific Research and the fellowship (Grant No. SFRH/BD/90410/2012) of J. Almeida are acknowledged as well.

References

1. C. G. Young, "A sun pumped CW one-watt laser," *Appl. Opt.* **5**(6), 993–997 (1966).
2. T. H. Dinh et al., "120 watt continuous wave solar-pumped laser with a liquid light-guide lens and an Nd:YAG rod," *Opt. Lett.* **37**(13), 2670–2672 (2012).
3. D. Liang and J. Almeida, "Solar-pumped TEM_{00}-mode Nd:YAG laser," *Opt. Express* **21**(21), 25107–25112 (2013).
4. D. Liang et al., "High-efficiency solar-pumped TEM_{00}-mode Nd:YAG laser," *Sol. Energ. Mater. Sol. Cells* **145**, 397–402 (2016).
5. D. Liang et al., "Solar-pumped Nd:YAG laser with 31.5 W/m^2 multimode and 7.9 W/m^2 TEM_{00}-mode collection efficiencies," *Sol. Energ. Mater. Sol. Cells* **159**, 435–439 (2017).
6. C. Zhao, Z. Guan, and H. Zhang, "How to harvest efficient laser from solar light," *Proc. SPIE* **10511**, 105111N (2018).
7. D. Liang et al., "Solar-pumped Cr:Nd:YAG ceramic laser with 6.7% slope efficiency," *Sol. Energy Mater. Sol. Cells* **185**, 75–79 (2018).

8. D. Liang et al., "Seven-rod pumping approach for the most efficient production of TEM_{00} mode solar laser power by a Fresnel lens," *J. Solar Energy Eng.* **143**, 061004 (2021).
9. T. Yabe et al., "Experimental study of solar pumped laser for magnesium-hydrogen energy cycle," *J. Phys: Conf. Ser.* **112**, 042072 (2008).
10. M. Lando et al., "Solar-pumped solid state laser program," *Proc. SPIE* **3110**, 196–201 (1997).
11. T. Yabe et al., "Demonstration of solar-pumped laser-induced magnesium production from magnesium oxide," in *Magnesium Technology*, S. N. Mathaudhu et al., Eds., pp. 55–58, Springer, Cham (2012).
12. T. Yabe et al., "Demonstrated fossil-fuel-free energy cycle using magnesium and laser," *Appl. Phys. Lett.* **89**(26), 261107–261123 (2006).
13. Z. Guan et al., "Demonstration of a free-space optical communication system using a solar-pumped laser as signal transmitter," *Laser Phys. Lett.* **14**(5), 055804 (2017).
14. G. Overton, "NOVEL LASERS: solar-pumped Nd:YAG lasers getting brighter," *Laser Focus World* **49** (2013).
15. M. Oliveira et al., "A path to renewable Mg reduction from MgO by a continuous-wave Cr:Nd:YAG ceramic solar laser," *Sol. Energy Mater. Sol. Cells* **155**, 430–435 (2016).
16. K. Hasegawa et al., "Solar-pumped laser and its application to energy conversion," in *Light, Energy and the Environ., OSA Tech. Digest (online)*, Optica Publishing Group (2014).
17. G. A. Landis, "Prospects for solar pumped semiconductor lasers," *Proc. SPIE* **2121**, 58–65 (1994).
18. M. A. Michael, "Wireless power transmission," *Int. J. Sci. Eng. Res.* **5**(10), 125 (2014).
19. S. T. Khanna and K. Sharma, "Laser technology improving wireless communication: a comprehensive study on laser communicator," *IOSR J. Comput. Eng.* **19**(4), 26–33 (2017).
20. F. Steinsiek et al., "Wireless power transmission technology development and demonstrations," in *Proc. 2nd Int. Conf. Recent Adv. in Space Technol.*, pp. 140–149 (2005).
21. T. Strite et al., "Fiber lasers: multiple laser beam materials processing," Laser Focus World, 2016, https://www.laserfocusworld.com/lasers-sources/article/16547084/fiber-lasers multiple-laser-beam-materials-processing
22. S. Eifel and J. Holtkamp, "Multi-beam technology boosts cost efficiency," Industrial Laser Solutions, 2013, https://www.industrial-lasers.com/micromachining/article/16485583/multibeam-technologyboosts-cost-efficiency
23. A. Gillner et al., "High power laser processing with ultrafast and multi-parallel beams," *J. Laser Micro/Nanoeng.* **14**(2), 129–137 (2019).
24. F. O. Olsen, K. S. Hansen, and J. S. Nielsen, "Multibeam fiber laser cutting," *J. Laser Appl.* **21**(3), 133–138 (2009).
25. A. Morace et al., "Enhancing laser beam performance by interfering intense laser beamlets," *Nat. Commun.* **10**(1), 1–9 (2019).
26. "Getting started using ZEMAX©," https://www.zemax.com
27. *LASCAD© – The Laser Engineering Tool*, LAS-CAD GmbH.
28. R. Boutaka et al., "A compact solar laser side-pumping scheme using four off-axis parabolic mirrors" *J. Russ. Laser Res.* **42**(4), 453–461 (2021).
29. J. Almeida, D. Liang, and E. Guillot, "Improvement in solar-pumped Nd:YAG laser beam brightness," *Opt. Laser Technol.* **44**(7), 2115–2119 (2012).
30. "Technical note: optical materials," https://www.newport.com/n/optical-materials (accessed 25 August 2022).
31. Z. Guan et al., "32.1 W/m^2 continuous wave solar-pumped laser with a bonding Nd:YAG/YAG rod and a Fresnel lens," *Opt. Laser Technol.* **107**, 158–161 (2018).
32. D. Liang et al., "Side-pumped continuous-wave Nd:YAG solar laser with 5.4% slope efficiency," *Sol. Energy Mater. Sol. Cells* **192**, 147–153 (2019).
33. D. Liang et al., "Simultaneous solar laser emissions from three Nd:YAG rods within a single pump cavity," *Sol. Energy* **199**, 192–197 (2020).
34. "Standard tables for reference solar spectral irradiances: direct normal, and hemispherical on 37° tilted surface," ASTM Standard G173–03 (2012).

35. Z. Bin et al., “The study of active medium for solar-pumped solid-state lasers,” *Acta Opt. Sin.* **27**, 1797–1801 (2007).
36. D. Liang and J. Almeida, “Highly efficient solar-pumped Nd:YAG laser,” *Opt. Express* **19**, 26399 (2011).
37. M. Weksler and J. Shwartz, “Solar-pumped solid-state lasers,” *IEEE J. Quantum Electron.* **24**(6), 1222–1228 (1988).
38. H. Arashi et al., “A solar-pumped CW 18W Nd:YAG laser,” *Jpn. J. Appl. Phys.* **23**(Part 1, No. 8), 1051–1053 (1984).
39. R. M. J. Benmair et al., “Solar-pumped Er, Tm, Ho:YAG laser,” *Opt. Lett.* **15**(1), 36–38 (1990).
40. D. Jenkins et al., “A solar-pumped Nd:YAG laser with a record efficiency of 4.7 W/m^2,” *Bull. Israel Phys. Soc.* **101**, 42 (1996).
41. T. Brand, “Compact 170-W continuous-wave diode-pumped Nd:YAG rod laser with a cusp-shaped reflector,” *Opt.Lett.* **20**(17), 1776–1778 (1995).
42. W. Koechner, *Solid-State Laser Engineering*, 6th ed., Springer, Berlin (1999).
43. M. Catela et al., “Renovating electrical power-to-TEM_{00} mode laser power conversion efficiency with four-lamp/four-rod pumping scheme,” *J. Mod. Opt.* **68**(17), 895–905 (2021).

Rabeh Boutaka is a PhD student in the Radiation Physics Department, Faculty of Physics, University of Sciences and Technology Houari Boumediene, Bab Ezzouar, Algiers. He joined Professor Liang’s lab in 2020 to work on solar-pumped lasers, focusing on numerical optimizations of solid-state solar-pumped lasers.

Dawei Liang is an associate professor in Physics Department of NOVA University of Lisbon. His research on solar-pumped lasers has been highlighted by editors of *CSP Today* and *Spotlight on Optics* in 2012, *Laser Physics* in 2013, and *Laser Focus World* in 2013 and 2016. Previous research was published in *Journal of Photonics for Energy* in 2019, 2020, and 2021. His team signed a book publishing contract on Solar-Pumped Lasers with Springer Nature in 2020. He was listed by Stanford University among World’s Top 2% Scientists in 2021.

Abdelhamid Kellou is a professor in the Radiation Physics Department, Faculty of Physics, University of Sciences and Technology Houari Boumediene, Bab Ezzouar, Algiers, and he is member of Quantum Electronics Laboratory (LEQ). He received his PhD in 1999. His research is focused on the dynamical behaviors of lasers and its applications, holography, and nonlinear optics. He is the author of more than twenty journal papers and director of several PhD theses.